

On the reflectance spectroscopy of snow

Alexander Kokhanovsky(1), Maxim Lamare(2,3), Biagio Di Mauro(4), Ghislain Picard (2), Laurent Arnaud (2), Marie Dumont (3), François Tuzet (3,2), Carsten Brockmann(5), Jason E. Box(6)

(1) VITROCISSET, Bratustrasse 7, D-64293 Darmstadt, Germany

(2) UGA, CNRS, Institut des Géosciences de l'Environnement (IGE), UMR 5001,
Grenoble, 38041, France

(3) Meteo-France–CNRS, CNRM UMR 3589, Centre d'Etudes de la Neige, Grenoble, France

(4) Department of Earth and Environmental Sciences, University of Milano-Bicocca, Piazza della Scienza, 1 20126 Milan, Italy

(5) Brockmann Consult, Max Planck Strasse 2, Geesthacht, Germany

(6) Geological Survey of Denmark and Greenland (GEUS), Copenhagen, Denmark

Abstract

We propose a system of analytical equations to retrieve snow grain size and absorption coefficient of pollutants from snow reflectance or snow albedo measurements in the visible and near-infrared regions of the electromagnetic spectrum, where snow single scattering albedo is close to 1.0. It is assumed that ice grains and impurities (e.g., dust, black and brown carbon) are externally mixed, the snow layer is semi-infinite and vertically and horizontally homogeneous. The influence of close-packing effects on reflected light intensity are assumed to be small and ignored. The system of nonlinear equations is solved analytically in the assumption that impurities have the spectral absorption coefficient, which obey the Angström power law, and the impurities influence the registered spectra only in the visible and not at near-infrared (and vice versa for ice grains). The theory is validated using spectral reflectance measurements and albedo of clean and polluted snow at various locations (Antarctica Dome C, European Alps). The technique to derive the snow albedo (plane and spherical) from

reflectance measurements at a fixed observation geometry is proposed. The technique also enables the simulation of hyperspectral snow reflectance measurements in the broad spectral range from ultraviolet to the near-infrared for a given snow surface in the case, if the actual measurements are performed at restricted number of wavelengths (2-4, depending on the type of snow and the measurement system).

34

35

36 1. Introduction

37 The reflective properties of clean and polluted snow are of importance for various applications
38 including climate (Hansen and Nazarenko, 2007) and environmental pollution (Nazarenko et al.,
39 2017) studies. The spectral snow reflectance is usually studied in the framework of the radiative
40 transfer theory. The application of the numerical methods for the solution of the radiative
41 transfer equation for snow layers has been performed by Mishchenko et al. (1999), Stamnes et al.
42 (2011), and He et al. (2018) among others. The approximate solutions of the radiative transfer
43 equation useful for snow optics and spectroscopy applications have been developed by Warren
44 and Wiscombe (1980), Wiscombe and Warren (1980) and Kokhanovsky and Zege (2004). In this
45 work, we propose an analytical snow albedo and reflectance model, which can be used to derive
46 near - surface snow optical and microphysical properties using measurements at just two to four
47 wavelengths in the visible and near-infrared depending on the measurement system and type of
48 snow. In particular, we present the method for the determination of snow grain size, absorption
49 Angström coefficient and spectral absorption coefficient of impurities embedded in the snow
50 matrix assuming an external mixture of snow grains and impurities. A technique to derive the
51 snow albedo from reflectance measurements is also presented. The absorption and extinction of
52 light by snow grains is treated in the framework of a geometrical optical approximation. The
53 absorption coefficient of impurities is modeled using the Angström power law. All derivations

54 are performed in the framework of the asymptotic radiative transfer theory (see, e.g.,
55 Kokhanovsky and Zege, 2004, Zege et al., 2011). It is assumed that the snow layer is vertically
56 and horizontally homogeneous and semi-infinite. Therefore, the effects of the finite layer
57 thickness are ignored.

58

59 **2. Theory**

60 **2.1 The snow reflectance**

61 The snow reflectance R (equal to unity for ideal white Lambertian reflectors, see Appendix A)
62 can be presented in the following way using approximate asymptotic radiative transfer theory
63 (Kokhanovsky and Zege, 2004):

64
$$R = R_0 r_s^x, \quad (1)$$

65 where $x = u(\mu_0)u(\mu)/R_0$, R_0 is the reflectance of a semi-infinite non-absorbing snow layer,
66 $u(\mu_0) = \frac{3}{7}(1+2\mu_0)$, μ_0 is the cosine of the solar zenith angle, μ is the cosine of the viewing
67 zenith angle, r_s is the snow spherical albedo:

68
$$r_s = e^{-y}, \quad (2)$$

69 where

70
$$y = 4 \sqrt{\frac{1-\omega_0}{3(1-g)}}, \quad (3)$$

71 g is the asymmetry parameter, ω_0 is the single scattering albedo. Let us introduce the probability
 72 of photon absorption $\beta \equiv 1 - \omega_0$. It is equal as the ratio of absorption κ_{abs} and extinction κ_{ext}
 73 coefficients:

$$74 \quad \beta = \frac{\kappa_{abs}}{\kappa_{ext}}, \quad (4)$$

75 where

$$76 \quad \kappa_{abs} = \kappa_{abs}^{ice} + \kappa_{abs}^{pol}. \quad (5)$$

77 The first and second terms in Eq. (5) correspond to the ice grains and pollutants, respectively.
 78 We assume that scattering and extinction of light by impurities is much smaller than that by ice
 79 grains and, therefore (Kokhanovsky and Zege, 2004),

$$80 \quad \kappa_{ext} = \frac{3c}{d}. \quad (6)$$

81 Here, $d = 1.5\bar{V}/\bar{S}$ is the effective diameter of ice grains, \bar{V} is the average volume of grains, \bar{S}
 82 is their average projected area averaged over all directions (equal to $\sum/4$ for convex particles in
 83 random orientation, where \sum is the average surface area and c is the volumetric concentration of
 84 the snow grains). The value of c is equal to the volume of grains in unit volume of snow
 85 ($c = N\bar{V}$, where N is the number of snow grains in unit volume of snow (cm^{-3})). It is related to
 86 the dry snow density ρ_s by the following relation: $\rho_s = c\rho_i$, where ρ_i is the bulk ice density.

87 The product of the effective diameter d and the bulk ice absorption coefficient α is a small
 88 number in the visible and near-infrared. Then it follows (Kokhanovsky and Zege, 2004, see their
 89 Eq. (37) for the absorption path length inversely proportional to the absorption coefficient) that:

90
$$\kappa_{abs}^{ice} = B\alpha c, \quad (7)$$

91 where B is the grain shape-dependent parameter (absorption enhancement parameter),
 92 $\alpha = \frac{4\pi\chi}{\lambda}$, where χ is the imaginary part of the ice refractive index at the wavelength λ .

93 We present the absorption coefficient of pollutants in snow as

94
$$\kappa_{abs}^{pol}(\lambda) = \kappa_0 \tilde{\lambda}^{-m}, \quad (8)$$

95 where $\kappa_0 \equiv \kappa_{abs}^{pol}(\lambda_0)$, $\tilde{\lambda} = \lambda / \lambda_0$, $\lambda_0 = 1 \mu m$, m is the absorption Angstrom coefficient.

96 It follows from Eqs. (4)-(8):

97
$$\beta = \frac{B\alpha d}{3} + \beta^{pol}, \quad (9)$$

98 where

99
$$\beta^{pol} = \frac{\kappa_0 \tilde{\lambda}^{-m} d}{3c} \quad (10)$$

100 and therefore:

101
$$y = \frac{4}{3} \sqrt{\frac{(B\alpha + \kappa_0 \tilde{\lambda}^{-m} c^{-1})d}{1-g}}. \quad (11)$$

102 Let the parameter $z = y^2$, from which it follows that:

103
$$z = (\alpha + f \tilde{\lambda}^{-m})l, \quad (12)$$

104 where

105
$$f = \frac{\kappa_0^*}{B}, \quad (13)$$

106 $\kappa_0^* = \kappa_0 / c$ and

107
$$l = \xi d \quad (14)$$

108 is the effective absorption length (EAL) and

109
$$\xi = \frac{16B}{9(1-g)} \quad (15)$$

110 is a grain shape (but not the grain size) dependent parameter.

111 The parameter l can be determined directly from reflectance or albedo measurements, enabling

112 also the determination of the grain diameter $d = l / \xi$ assuming a particular shape of grains. It has

113 been found that the asymmetry parameter of crystalline clouds is usually in the range 0.74-0.76

114 in the visible (Garret, 2008). The asymmetry parameter g for snow has not been measured so far

115 *in situ* but we shall assume that it is close to that in crystalline clouds and adopt the value 0.75. It

116 follows from experimental studies of Libois et al. (2014) that $B=1.6$ on average. Therefore, it

117 follows (see Eq. 15): $\xi \approx 11.38$.

118 Using the EAL, the equations for the snow reflectance and spherical albedo may be simplified.

119 Namely, it follows:

120
$$R = R_0 \exp(-x \sqrt{(\alpha + f \tilde{\lambda}^{-m})l}), \quad (16)$$

121
$$r_s = \exp(-\sqrt{(\alpha + f \tilde{\lambda}^{-m})l}). \quad (17)$$

122 The plane albedo can be derived as well (Kokhanovsky and Zege, 2004):

123
$$r = \exp(-u(\mu_0) \sqrt{(\alpha + f \tilde{\lambda}^{-m})l}). \quad (18)$$

124 The relationship between the albedo and the reflectance R is given in Appendix A. It follows
 125 from Eq. (16) that the spectral reflectance of polluted snow is determined by four *a priori*
 126 unknown parameters: l, R_0, f, m . They can be estimated from the measurements of reflectance at
 127 four wavelengths. This also enables the determination of the spectral reflectance (and albedo, see
 128 Eq.(18)) at the visible and near – infrared wavelengths at an arbitrary λ . It follows:

129
$$R_1 = R_0 \exp(-x \sqrt{(\alpha_1 + f \tilde{\lambda}_1^{-m})l}), \quad (19)$$

130
$$R_2 = R_0 \exp(-x \sqrt{(\alpha_2 + f \tilde{\lambda}_2^{-m})l}) \quad (20)$$

131
$$R_3 = R_0 \exp(-x \sqrt{(\alpha_3 + f \tilde{\lambda}_3^{-m})l}) \quad (21)$$

132
$$R_4 = R_0 \exp(-x \sqrt{(\alpha_4 + f \tilde{\lambda}_4^{-m})l}) \quad (22)$$

133 where the numbers 1, 2, 3, and 4 signify the wavelengths used. Equations (19)-(22) can be used
 134 to compute four unknown parameters given above, and, therefore, determine reflectance and
 135 albedo at any wavelength in the visible and the near-infrared using Eqs. (16)-(18). Let us assume
 136 that the spectral channels are selected in a way that the effects of ice absorption can be neglected
 137 in the first two channels (λ_1, λ_2) and effects of absorption by pollutants are negligible in the
 138 second pair of channels (λ_3, λ_4). This situation is typical of not heavily polluted snow. Then it
 139 follows instead of Eqs. (19)-(22):

140
$$R_1 = R_0 \exp(-x \sqrt{f \tilde{\lambda}_1^{-m} l}), \quad (23)$$

141
$$R_2 = R_0 \exp(-x\sqrt{f\tilde{\lambda}_2^{-m}l}), \quad (24)$$

142
$$R_3 = R_0 \exp(-x\sqrt{\alpha_3 l}), \quad (25)$$

143
$$R_4 = R_0 \exp(-x\sqrt{\alpha_4 l}). \quad (26)$$

144 Eqs. (25), (26) can be used to find the pair (l, R_0) :

145
$$R_0 = R_3^{\varepsilon_1} R_4^{\varepsilon_2}, \quad l = \frac{1}{x^2 \alpha_4} \ln^2 \left[\frac{R_4}{R_0} \right], \quad (27)$$

146 where $\varepsilon_1 = 1/(1-b)$, $\varepsilon_2 = 1/(1-b^{-1})$, $b = \sqrt{\alpha_3 / \alpha_4}$. Then it follows from Eqs. (23), (24) that:

147
$$m = \frac{\ln(p_1 / p_2)}{\ln(\lambda_2 / \lambda_1)}, \quad (28)$$

148
$$f = \frac{p_1 \tilde{\lambda}_1^m}{x^2 l}, \quad (29)$$

149 where $p_k = \ln^2(R_k / R_0)$. In case of the absence of pollutants, Eqs. (27) remain valid. However,

150 the parameters m and f are undefined and $R = R_0 \exp(-x\sqrt{\alpha l})$.

151 One may also derive the impurity absorption coefficient at the wavelength
 152 λ_0 normalized to the concentration of ice grains c (see Eq. (13)):

153
$$\kappa_0^* = Af, \quad (30)$$

154 where f is given by Eq.(29). The normalized absorption coefficient at each wavelength can also
 155 be found using Eqs. (8), (28), (30).

156 To determine the concentration of pollutants (c_p) one must either know in advance or determine
 157 the impurity volumetric absorption coefficient defined as:

$$158 \quad K(\lambda_0) = \frac{\bar{C}_{abs}(\lambda_0)}{\bar{V}}, \quad (31)$$

159 where \bar{C}_{abs} is the average absorption cross section of impurities and \bar{V} is the average volume of absorbing
 160 impurities. Namely, it follows by definition:

$$161 \quad c_p = \frac{\kappa_0}{K(\lambda_0)} \quad (32)$$

162 and

$$163 \quad \mathbb{C} = \frac{\kappa_0^*}{K(\lambda_0)}, \quad (33)$$

164 where $\mathbb{C} = c_p / c$.

165 The value of $K(\lambda_0)$ can be found, if one knows the type of pollutants and their microphysical properties.
 166 In particular, it follows for the impurities much smaller than the wavelength λ_0 (van de Hulst, 1981) that :

$$167 \quad K(\lambda_0) = F \alpha_{pol}(\lambda_0), \quad (34)$$

168 where

$$169 \quad \alpha_{pol}(\lambda_0) = \frac{4\pi\chi_{pol}(\lambda_0)}{\lambda_0} \quad (35)$$

170 is the pollutant bulk absorption coefficient, $\chi_{pol}(\lambda_0)$ is the imaginary part of pollutant refractive
 171 index and n_{pol} is the real part of the pollutant refractive index,

172

$$F = \frac{9n_{pol}}{\left(n_{pol}^2 + 1 - \chi_{pol}^2\right)^2 + 4n_{pol}^2\chi_{pol}^2} . \quad (36)$$

173 It follows that $F = 0.9$ for soot (assuming that $n=1.75$, $\chi_{pol} = 0.47$ in the visible). One can see
 174 that \mathbb{C} can be found if one knows the refractive index of absorbing Rayleigh particles in
 175 advance.

176 In particular, it follows for soot impurities that:

177

$$\mathbb{C} = \frac{Ap_1\tilde{\lambda}_1^m}{x^2lF\alpha_{pol}(\lambda_0)} . \quad (37)$$

178 In case of non-Rayleigh scatterers, one needs to know not only the refractive index but
 179 also the particle size distribution and shape of particles, enabling the determination of the
 180 impurity volumetric absorption coefficient $K(\lambda_0)$ and, therefore, the normalized concentration
 181 of impurities

182

$$\mathbb{C} = \frac{Ap_1\tilde{\lambda}_1^m}{x^2lK(\lambda_0)} . \quad (38)$$

183

184

2.2. The snow albedo

2.2.1 Theory

187 If the plane albedo is the measured physical quantity one needs to find only three constants:

188 l, f, m .

189 The respective analytical equations can be presented as:

$$190 \quad r_1 = \exp(-u(\mu_0) \sqrt{(\alpha_1 + f \tilde{\lambda}_1^{-m})l}), \quad (39)$$

$$191 \quad r_2 = \exp(-u(\mu_0) \sqrt{(\alpha_2 + f \tilde{\lambda}_2^{-m})l}), \quad (40)$$

$$192 \quad r_3 = \exp(-u(\mu_0) \sqrt{(\alpha_3 + f \tilde{\lambda}_3^{-m})l}). \quad (41)$$

193 We shall assume that the last channel is not influenced by impurities and the first two channels

194 are not influenced by the absorption of light by grains. Then it follows that:

$$195 \quad r_1 = \exp(-u(\mu_0) \sqrt{f \tilde{\lambda}_1^{-m} l}), \quad (42)$$

$$196 \quad r_2 = \exp(-u(\mu_0) \sqrt{f \tilde{\lambda}_2^{-m} l}), \quad (43)$$

$$197 \quad r_3 = \exp(-u(\mu_0) \sqrt{\alpha_3 l}). \quad (44)$$

198 The EAL can be found from Eq. (44):

$$199 \quad l = \frac{\ln^2 r_3}{u^2(\mu_0) \alpha_3}. \quad (45)$$

200 It follows from Eqs. (42), (43) that:

201

$$m = \frac{\ln(\psi_2 / \psi_1)}{\ln(\lambda_1 / \lambda_2)}, f = \frac{\psi_1 \tilde{\lambda}_1^m}{u^2(\mu_0)l}, \quad (46)$$

202 where $\psi_k = \ln^2 r_k$.

203 In case of unpolluted snow, one derives:

204

$$r = \exp(-u(\mu_0)\sqrt{\alpha l}). \quad (47)$$

205 Eq. (45) can be used to find the effective absorption length and, therefore, the spectral albedo of
206 unpolluted snow at any wavelength using Eq. (47). If not plane but rather spherical albedo is
207 measured, then all equations presented in this section are valid except one should assume that
208 $u=1$ and substitute r by r_s (Kokhanovsky and Zege, 2004).

209 **3. Experiment**

210 **3.1 The measurements of the plane albedo**

211 We have applied the technique developed above to the measured spectral plane albedo both for
212 polluted and pure snow. Therefore, in-situ spectral albedo measurements were obtained from two
213 different field sites located in the French Alps (polluted snow) and in Antarctica (clean snow).

214 The spectral albedo of a spring alpine snowpack was measured at the Col du Lautaret field site
215 (45°2' N, 6°2' E, 2100 m a.s.l.) in the French Alps. The measurements were performed using a
216 non-automated version of the spectrometer system described above. The hand-held instrument
217 has a single light collector, located at the end of 3 m boom placed 1.5 m above the surface. The
218 boom is rotated by the operator to successively acquire the downward and upward solar

219 radiation. The spectral albedo data (each spectral albedo measurement at a given point is an
220 average of five measurements) at several locations close to the location Col du Lautaret field site
221 was obtained on 12th April, 2017 across a 100 m transect, in attempt to account for spatial
222 variability. The measurements were acquired in clear sky conditions, with a solar zenith angle
223 varying between 47.9° and 52.2°.

224 The results of comparison of measurements and the theory presented above are illustrated in
225 Fig.1 at the Col du Lautaret field site. The parameters l, f, m have been found from Eqs. (42)-
226 (44) and the measurements at the wavelengths $\lambda_1 = 400\text{nm}$, $\lambda_2 = 560\text{nm}$, $\lambda_3 = 1020\text{nm}$. At other
227 measurement sites across a transect the results of the inter-comparison are excellent and similar
228 to that presented in Fig.1. Therefore, the theory can be used to derive snow optical and
229 microphysical properties even for polluted snowpack. The derived spectral probability of photon
230 absorption for the case shown in Fig. 1 is presented in Fig.2. The derived absorption coefficient
231 (assuming $c=1/3$), the grain diameter d and the absorption Angström parameter m for five sites
232 across the transect are listed in Table 1 (lines 1-5). It follows that the value of m is in the range
233 2.4 - 4.1 consistent with the identified presence of dust particles in snow (Doherty et al., 2010).
234 The pure black carbon impurities have the values of m close to one. The grain diameter is in the
235 range 1.7-2.2 mm consistent with low values of snow albedo at 1020nm (see Fig.1). Wiscombe
236 and Warren (1981) have calculated the dependence of the clean snow spectral albedo at the solar
237 zenith angle 60 degrees and several grain radii and presented it in their Fig.8. It follows from
238 their calculations that the albedo decreases from 0.8 to 0.4 while the diameter of grains changes
239 from 0.1 to 2mm. It follows from our Fig.1 that the measured plane albedo is close to 0.45
240 signifying the dominance of large grains in the snowpack as reported in Table 1.

241 The spectral albedo of pure snow (very low amount of impurities) was measured at Dome C
242 ($75^{\circ}5' S$, $123^{\circ}17' E$), in Antarctica using an automated spectral radiometer (Libois et al., 2015;
243 Picard et al., 2016; Dumont et al., 2017). The instrument is composed of two individual heads
244 located approximately 1.5 m above the surface. Each head contains two cosine receptors facing
245 upward and downward, which receive the incident solar radiation and the reflected radiation. The
246 collectors are connected to a MAYA2000 PRO Ocean Optics spectrometer with fibre optics
247 through an optical switch. Radiation is measured over 350-2500 nm spectral range with an
248 effective spectral resolution of 3 nm. Albedo was calculated as the ratio of the upward and
249 downward spectral irradiance. The full description of the instrument and the processing steps to
250 calculate the spectral albedo are given by Picard et al. (2016). The spectral albedo measurements
251 used here were made on the 10th January 2017, with a solar zenith angle of 63.2° , during clear
252 sky conditions assessed by ground observations.

253 The results of the application of the proposed technique to the pure snow (no pollution) albedo
254 measured in Antarctica are illustrated in Fig.3. Application of our technique results in excellent
255 agreement with measured albedo over pure snow (now pollution) in Antarctica. Because the
256 snow at Dome C is clean/pristine, the value of f is negligible, resulting in snow albedo depending
257 only on the effective absorption length/grain size, which has been derived at a single wavelength
258 (1020nm). The derived grain diameter for the case presented in Fig.3 is equal to 0.5mm. The
259 retrieval error estimation is presented in Appendix B.

260

261

262

263 **3.2 The measurements of the spectral reflectance**

264 The application of the developed theory to the measurements of the spectral reflectance is
265 presented in Fig.4 for two locations with different dust loads (39.6ppm and 107.4ppm). The
266 spectral reflectance of snow was measured in the European Alps (Artavaggio plains, 1650m
267 a.s.l., $45^{\circ}55'56.70''$ N; $9^{\circ}31'33.28''$ E) at the solar zenith angle equal to 52 degrees. The
268 measurements were made on March 14th 2014, after a major transport and deposition of mineral
269 dust from the Saharan desert. The event was very intense, and it was reported in the recent
270 scientific literature regarding snow optical properties, (Di Mauro et al., 2015; Dumont et al.,
271 2017), atmospheric chemistry and physics (Belosi et al., 2017), and also microbiology (Weil et
272 al., 2017). The dust transport event deposited fine mineral dust particles from the atmosphere via
273 wet deposition, according to the BSC-DREAM-8b model (Basart et al., 2012). Spectral
274 measurements of snow were made using a field spectrometer (Field Spec Pro, Analytical
275 Spectral Devices, ASD). This instrument features a spectral range of 350-2500 nm, a full width
276 at half maximum of 5–10 nm, and a spectral resolution of 1 nm. Data presented here were
277 collected under clear sky conditions at noon. Incident radiation was estimated using a
278 Lambertian Spectralon panel. Reflected radiance was divided by incident radiance, and the
279 hemispherical conical reflectance factor was calculated for two plots containing 39.6 and 107.4
280 ppm of dust. Dust concentration was measured with a Coulter Counter by integrating particles
281 with a diameter smaller than 18 μ m. Spectral measurements were performed at nadir using a bare
282 optical fiber (field of view of 25°) at 80 cm from the snow sample. Both the optical fiber and the
283 spectralon panel were equipped with an optical level. Further details on this dataset can be found
284 in Di Mauro et al. (2015).

285 One can see that the theory works well not only for the albedo measurements (see the
 286 previous section) but also for the reflectance measurements for polluted snow layers. In
 287 particular, our results are closer to the measurements as compared to the theoretical model
 288 described by Flanner et al. (2007) (see Fig.4b in Di Mauro et al., 2015). The derived parameters
 289 are given in Table 1 (lines 6-7). The value of m is 4.1 for the case with the 39.6ppm dust
 290 concentration and it is 6.4 for the case with 107.4 dust concentration. Because the difference is
 291 quite large for the close locations we conclude that snow also contained other pollutants (say,
 292 soot) and the determined value of m represents the combined effect with larger values of m for
 293 larger concentrations of dust, which is consistent with other observations of this parameter in
 294 snow (Doherty et al., 2010). The retrieved absorption coefficient of snow pollutants (at the
 295 wavelength $\lambda^* = 560nm$) is $0.1191 m^{-1}$ for the dust concentration 39.6ppm and it is $0.3123 m^{-1}$
 296 for the dust concentration of 107.4 ppm. Assuming that the dust chemical composition and also
 297 the dust particle size distribution are the same at both locations we can assume that the ratio of
 298 absorption coefficients at two locations should be equal to the ratio of dust concentrations. The
 299 difference between the two ratios is $<3\%$, which is within the measurement uncertainty (10% for
 300 dust load measurements), and suggesting that the retrieved absorption coefficients at the two
 301 sites are consistent with each other.

302 The mass absorption coefficient (MAC) can be estimated using:

303

$$K_m = \frac{\kappa_{abs}^{pol}(\lambda^*)}{C\rho c}, \quad (48)$$

304 where ρ is the density of the substance of impurities. Assuming that:

305

$$\rho = 2.62 g / cm^3 \text{ (as for quartz), } c = 1/3, \quad C = 107.4 ppm \text{ and } \kappa_{abs}^{pol}(\lambda^*) = 0.3123 m^{-1}, \quad (49)$$

306 one can derive that:

307
$$K_m = 0.0033m^2 / g, \quad (50)$$

308 which is consistent with the values of MAC given by Utry et al.(2015) (e.g.,

309 $0.0023m^2 / g$ for quartz and $0.0051m^2 / g$ for illite (see their Table 1)).

310 **4. Conclusions**

311 In this work, we have presented a sequence of analytical equations, which can be used to
312 determine the snow grain size, the absorption coefficient of impurities, and the absorption
313 Angström coefficient of surface snow impurities from the snow reflectance measured at four
314 wavelengths: two in the visible and two in the near infrared as suggested by Warren (2013). In
315 the case of albedo measurements just three wavelengths can be used to find main snow
316 properties. For unpolluted snow, it is enough to perform the measurements at two wavelengths
317 (for reflectance measurements) or just at a single wavelength (for albedo measurements) in the
318 near-infrared to determine the snow grain size.

319 In principle, the refractive index of dust and dust size distribution can be also determined using
320 derived spectral absorption coefficient of dust and assuming the shape of dust particles.
321 However, we did not make an attempt for such retrievals in this work. The method for the
322 retrieval of the complex refractive index and single scattering optical properties of dust deposited
323 in mountain snow based on exact radiative transfer calculations has been proposed by McKenzie
324 Siles et al. (2016) in the assumption that local optical properties of dust grains can be simulated
325 assuming the spherical shape of particles. Their method is based on the extraction of dust grains
326 from snowpack. Our technique does not require such a complicated procedure.

327 We have demonstrated how snow albedo can be derived from spectral reflectance measurements
328 avoiding complicated integration with respect to the observation geometry (azimuth, viewing
329 angle). The last point is useful for the determination of the snow *albedo* from spectral *reflectance*
330 measurements (say, from aircraft or satellite) at a fixed observation geometry. Although the
331 comprehensive validation of the retrievals has not been attempted, we have found that the ratio
332 of derived absorption coefficients of pollutants at two concentrations is close to the ratio of
333 pollutant concentrations derived independently, which indeed should be the case taking the
334 proximity of two measurement sites with different dust loads. The general validity of the
335 approach is proven using field measurements (Alps, Antarctica) of both spectral reflectance and
336 plane albedo.

337 The determination of the EAL l (unlike the effective grain diameter d) both from reflectance
338 and albedo measurements is practically insensitive to *apriori* unknown shape of ice crystals.
339 Therefore, this length may be useful for the characterization of snowpack microstructure (in
340 addition to the grain size d). The results presented in this work are useful for the interpretation of
341 snow properties using both reflectance spectroscopy (Hapke, 2005) and imaging spectrometry
342 (Dozier et al., 2009). It is assumed that the semi - infinite snow layer is vertically and
343 horizontally homogeneous. The effects of the snow layer finite thickness, close packing effects,
344 snow vertical inhomogeneity, possible internal mixture of pollutants in snow grains, and
345 underlying surface albedo (ice, soil, grass) are ignored.

346

347

348

350 **Appendix A. Nomenclature**

Physical parameter	Notation	Units	Definition	Comments
Snow absorption coefficient	κ_{abs}	m^{-1}	$N\bar{C}_{abs}$	N -number of snow grains in unit volume(m^{-3}) \bar{C}_{abs} -average absorption cross section of grains (m^2)
Snow extinction coefficient	κ_{ext}	m^{-1}	$N\bar{C}_{ext}$	N -number of snow grains in unit volume(m^{-3}) \bar{C}_{ext} -average extinction cross section of grains (m^2)
Probability of photon absorption	β	-	$\kappa_{abs} / \kappa_{ext}$	$\beta \ll 1$ in the approximation studied
Snow single scattering albedo	ω_0	-	$1-\beta$	close to 1 in the approximation studied
Snow asymmetry parameter	g	-	$g = \frac{1}{2} \int_0^\pi p(\theta) \sin \theta \cos \theta d\theta$	$\frac{1}{2} \int_0^\pi p(\theta) \sin \theta d\theta = 1$ θ is the scattering angle(equal to π in the exact backward scattering direction) $p(\theta)$ is the conditional probability of photon scattering in a given direction specified by the angle θ (phase function)
Bulk ice absorption coefficient	α	m^{-1}	$\frac{4\pi\chi(\lambda)}{\lambda}$	$\chi(\lambda)$ - imaginary part of bulk ice refractive index λ - wavelength
Volumetric absorption coefficient of pollutants	K	m^{-1}	$\bar{C}_{abs}^{pol} / \bar{V}_p$	\bar{C}_{abs}^{pol} -average absorption cross section of impurities in snow (m^2), \bar{V}_p is their average volume(m^3), K is <u>proportional</u> to the bulk absorption coefficient of impurities in case they are much larger as compared to

				the wavelength (and weakly absorbing) or much smaller as compared to the wavelength (so called Rayleigh scatterers). The coefficient of proportionality (absorption enhancement factor) depends on the shape of particles and real part of their complex refractive index.
Effective absorption length	l	m^{-1}	$\frac{\ln^2 r_s}{\alpha}$ (for clean dry snow)	$r_s = \exp(-\sqrt{\alpha}l)$ r_s -spherical albedo α -bulk ice absorption coefficient This definition holds for clean dry snow only The general definition for dry snow is given by Eq. (17)
Reflectance	$R(\mu_0, \mu, \varphi)$	-	$I^\uparrow(\mu_0, \mu, \varphi) / I_{Lamb}^\uparrow(\mu_0)$	Ratio of intensity of light reflected from a given snowpack to that of an ideal Lambertian surface with albedo 1.0 (μ_0, μ, φ) -cosine of the solar zenith angle, cosine of viewing zenith angle, and relative azimuth, respectively
Plane albedo	$r(\mu_0)$	-	$2 \int_0^1 \bar{R}(\mu_0, \mu, \varphi) \mu d\mu$	$\bar{R} = \frac{1}{2\pi} \int_0^\pi R(\mu_0, \mu, \varphi) \varphi d\varphi$ - reflectance averaged with respect to the azimuth, black sky albedo
Spherical albedo	r_s	-	$2 \int_0^1 r(\mu_0) \mu_0 d\mu_0$	white sky albedo
Volumetric concentration of grains	c	-	$N\bar{V}$	N – number concentration of grains, \bar{V} -average volume of grains, c - fraction of unit volume occupied by ice grains (usually around 0.3)
Mass concentration of	ρ_s	gm^{-3}	$N\bar{m}$	N – number concentration of grains,

grains (snow density)				$\bar{m} = \rho_i \bar{V}$ -average mass of grains, ρ_i - bulk ice density, $\rho_s = \rho_i c$ (for dry snow)
Bulk ice density	ρ_i	gm^{-3}	-	$\rho_i = 916.7 kg / m^3$ at $0^\circ C$
Bulk pollutant density	ρ_p	gm^{-3}	-	
Volumetric concentration of impurities	c_p	-	$N_p \bar{V}_p$	N_p – number concentration of pollution particles, \bar{V}_p -average volume of pollution particles, c - fraction of unit volume occupied by impurities
Normalized volumetric concentration of impurities	\mathbb{C}	-	c_p / c	$\mathbb{C} = \frac{\rho_i}{\rho_s} c_p$ ρ_i - bulk ice density, ρ_s - snow density, c_p - volumetric concentration of impurities
Effective diameter of grains	d	m	$\frac{3\bar{V}}{2\bar{S}}$	equal to the diameter for the collection of spherical grains of the same size, \bar{V} -average volume of grains, \bar{S} -average cross section of grains (perpendicular to incident light beam),

351

352

353

354

355

356

357

358 **Appendix B. The retrieval error estimation**359 **1. The effective absorption length and diameter of grains**

360 Let us consider the error budget for the retrieved snow parameters. To simplify, we assume that
 361 the snow parameters are derived using albedo measurements.

362 The value of l is determined from measurements just at a single wavelength in the framework of
 363 the theory given above. It follows from Eq. (45):

$$364 \quad \frac{\Delta l}{l} = K \frac{\Delta r_3}{r_3}, \quad (B.1)$$

365 where

$$366 \quad K = \frac{2}{\ln r_3}. \quad (B.2)$$

367 Therefore, the relative effective absorption length retrieval error is directly proportional to the
 368 relative measurement error in the measured albedo. Larger values of l correspond to the smaller
 369 albedo. So one conclude that that the error of retrieval of larger values of EAL are generally
 370 smaller (see Eq.(B.2)). For the cases, presented in Figs. 1 and 2, the wavelength 1020nm has
 371 been used in the retrieval process and one finds that K is equal to -2.5 and -5.8, respectively.
 372 Assuming the measurement error of 3%, one derives that EAL is determined with the accuracy -
 373 7.5 and -17.4 %, respectively with better accuracy for the observations in Alps, because the
 374 albedo is lower there. Also we see that the overestimation of the albedo in the experiment leads
 375 to the underestimation of the EAL and other way around in case measurements which
 376 underestimate the snow albedo because K is negative. Because K generally decreases with the

377 wavelength one must use the largest wavelengths to have better accuracy (say, 1020nm instead
378 of 865nm). The wavelength should not be above 1200nm or so (depending on the snow grain
379 size) because the underlying theory valid for weakly absorbing media only. So strong ice
380 absorption bands must be avoided. The value of the snow grain size is proportional to the value
381 of l . Therefore, our conclusions are also valid for the derived snow grain size assuming that one
382 knows the parameter ξ (see Eq.15) exactly. However, this parameter is known with some error.

383 The uncertainty in the parameter $\xi = 16B / 3(1-g)$ is difficult to access because we rely on a priori
384 value for the snow asymmetry parameter and the absorption enhancement parameter B . We use
385 the following values: $B=1.6$, $g=0.75$. The reported values of g for for crystalline clouds do not
386 go above 0.8. Therefore, the module of the absolute error in the parameter $1-g$ is smaller than
387 0.05 (and the relative error is below 20%). The value of B is usually in the range: 1.4-1.8 and,
388 therefore, the absolute error in the parameter B is equal approximately to ± 0.2 and, therefore,
389 the relative error is $\pm 12.5\%$. It follows that the absolute value of the maximal relative error in
390 the parameter ξ is close to 24%. The error could be smaller in case the assumptions used in the
391 derivations are closer to the actual snow conditions. We find that the maximal relative error in
392 the derived grain diameter for the cases shown in Fig. 1, 2 is 25-30% depending on the snow
393 type, which is substantially larger as compared to the error in the estimation of EAL.

394

395

396

397

398 **2. The spectral absorption coefficient of pollutants**

399 Let us consider the error budget for the retrieved spectral absorption coefficient of
 400 pollutants. The absolute error of the retrieved parameter Δx is defined as

401
$$\Delta x = \sqrt{\sum_{j=1}^J \left[\frac{\partial x}{\partial y_j} \right]^2 \Delta y_j^2}. \quad (B.3)$$

402 This error depends on j measurement errors of reflectance/albedo at j -channel Δy_j , where J is
 403 the number of channels used to retrieve the corresponding parameter assuming that there are no
 404 forward model errors. It is a difficult task to estimate the forward model error theoretically. It
 405 depends on the specific type of snowpack.

406 It follows from Eqs. (46), (B.3) :

407
$$\frac{\Delta f}{f} = \sqrt{\Upsilon_1^2 \left[\frac{dr_1}{r_1} \right]^2 + \Upsilon_3^2 \left[\frac{dr_3}{r_3} \right]^2}, \quad \frac{\Delta m}{m} = \sqrt{\Pi_1^2 \left[\frac{dr_1}{r_1} \right]^2 + \Pi_2^2 \left[\frac{dr_2}{r_2} \right]^2}, \quad (B.4)$$

408 where

409
$$\Upsilon_n = \frac{2}{\ln r_n}, \quad \Pi_n = \frac{2}{\ln r_n \ln(\psi_2 / \psi_1)}. \quad (B.5)$$

410 We conclude that the errors of the pair (f, m) determination increase, if the selected wavelengths
 411 at two channels in the visible are too close and if the logarithm of albedo at selected channels is
 412 close to unity (say, weak concentration of pollutants for the channels in the visible). The albedo
 413 decreases for the cases with illumination closer to nadir. Therefore, to reduce errors one needs to
 414 use the measurements with larger deviations of Sun from the horizon direction.

415

The absorption coefficient of pollutants is given by the following equation (see Eqs. (8),

416

(13),(30)):

417

$$\kappa_{abs}^{pol} = Bcf \tilde{\lambda}^{-m}.$$

(B.6)

418

Therefore, one derives

419

$$\frac{\Delta \kappa_{abs}^{pol}}{\kappa_{abs}^{pol}} = \sqrt{\left[\frac{\Delta B}{B} \right]^2 + \left[\frac{\Delta f}{f} \right]^2 + \left[\frac{dc}{c} \right]^2 + \ln^2(\tilde{\lambda}) \left[\frac{\Delta m}{m} \right]^2}. \quad (B.7)$$

420

One concludes that the errors in the estimated snow volumetric concentration c (snow density,

421

see Appendix A), the absorption enhancement coefficient B , and also pair (f,m) must be

422

combined to estimate the total error in the retrieved spectral absorption coefficient of impurities

423

in snow. The errors are lower, if one is interested in the spectral absorption coefficient of

424

impurities normalized to its value at a specific wavelength defined as

425

$$\tilde{\kappa}_{abs}^{pol} \equiv \frac{\tilde{\kappa}_{abs}^{pol}(\lambda)}{\tilde{\kappa}_{abs}^{pol}(\lambda_*)}, \quad (B.8)$$

426

where λ_* is the selected wavelength (say, 550nm).

427

One derives for this coefficient:

428

$$\tilde{\kappa}_{abs}^{pol}(\lambda) \equiv \left(\frac{\lambda}{\lambda_*} \right)^{-m} \quad (B.9)$$

429

and, therefore, only the accuracy of the determination of absorption Angstroem exponent
 430 influences the result:

431

$$\frac{\Delta \kappa_{abs}^{pol}}{\kappa_{abs}^{pol}} = \ln(\lambda / \lambda_*)^{-m} \frac{\Delta m}{m}. \quad (\text{B.10})$$

432

An important point is the determination of concentration of pollutants in snow from optical
 433 remote sensing data. In principle the concentration of pollutants can be found, if the absorption
 434 coefficient of pollutants at a given wavelength is known. For instance, it follows by definition
 435 (see Eq. (31) for the definition of the volumetric absorption coefficient of impurities K):

436

$$c_p = \frac{\kappa_{abs}^{pol}(\lambda)}{K(\lambda)}.$$

437

Therefore, uncertainty in the derived or assumed value of K (or mass extinction coefficient
 438 $K_m = K / \rho_p$, where ρ_p is the density of the substance of a pollutant) influences the retrieval error
 439 in addition to uncertainty of the derived absorption coefficient of pollutants $\kappa_{abs}^{pol}(\lambda)$. One can see
 440 that the determination of the concentration of pollutants from optical remote sensing of
 441 snowpack is a very challenging task.

442

In particular, one finds that the positive bias in the measured albedo in the visible will lead to
 443 the underestimation of the concentration of pollutants (assuming that the grain size is exactly
 444 known). It should be pointed out that in most cases the concentration of pollutants is so small
 445 that it can not be assessed using optical instruments (change in reflectance is inside experimental

446

measurement error). This issue has been discussed by Zege et al. (2011) and Warren (2013).

447

Similar conclusions hold also if the reflectance (and not albedo) is the measured quantity.

448

449

5. Acknowledgments

450

This work was mainly supported by the European Space Agency in the framework of ESRIN

451

contract No. 4000118926/16/I-NB "Scientific Exploitation of Operational Missions (SEOM)

452

Sentinel-3 Snow (Sentinel-3 for Science, Land Study 1: Snow)". CNRM/CEN and IGE are part of

453

labex OSUG@2020. Measurements in the French Alps were funded by the ANRJCJ grant EBONI

454

16-CE01-0006 and at Dome C by ANR JCJC MONISNOW 1-JS56-005-01.

455

456 **References**

457 S. Basart, S., C. Pérez, S. Nickovic, E. Cuevas, and J. M. Baldasano, "Development and
458 evaluation of the BSC-DREAM8b dust regional model over Northern Africa, the Mediterranean
459 and the Middle East", *Tellus B*, vol. 64, 2012, doi:10.3402/tellusb.v64i0.18539, 2012.

460 F. Belosi, M. Rinaldi, S. Decesari, L. Tarozzi, A. Nicosia, A., and G. Santachiara, "Ground
461 level ice nuclei particle measurements including Saharan dust events at a Po Valley rural site
462 (San Pietro Capofiume, Italy)", *Atmospheric Research*, vol. 186, pp. 116–126,
463 <https://doi.org/10.1016/J.ATMOSRES.2016.11.012>, 2017.

464 B. Di Mauro, F. Fava, L. Ferrero, R. Garzonio, G. Baccolo, B. Delmonte, and R. Colombo,
465 "Mineral dust impact on snow radiative properties in the European Alps combining ground,
466 UAV, and satellite observations", *J. Geophys. Res. Atmos.*, vol. 120, pp. 6080–6097,
467 doi:10.1002/2015JD023287, 2015.

468 S. J. Doherty, S. G. Warren, T. C. Grenfell, A. D. Clarke, and R.E. Brandt, "Light-absorbing
469 impurities in Arctic snow", *Atmos. Chem. Phys.*, vol. 10, 11647–11680, 2010.

470 J. Dozier, R. O. Green, A. W. Nolin, and T. H. Painter, "Interpretation of snow properties from
471 imaging spectrometry", *Remote Sens. Env.*, vol. 113, pp. S25–S37, 2009.

472 M. Dumont, L. Arnaud, G. Picard, Q. Libois, Y. Lejeune, P. Nabat, and S. Morin, S. "In situ
473 continuous visible and near-infrared spectroscopy of an alpine snowpack". *The Cryosphere*,
474 vol. 11, N3, pp. 1091–1110, <https://doi.org/10.5194/tc-11-1091-2017>, 2017.

475 M. G. Flanner, C. S. Zender, J. T. Randerson, and P. J. Rash, "Present – day climate forcing and
476 response from black carbon in snow", *J. Geophys. Res. Atmos.*, vol.112, D11202, doi:
477 10.1029/2006JD008003, 2007.

478 T. J. Garrett, "Observational quantification of the optical properties of cirrus cloud", *Light*
479 *Scattering Reviews* (ed. by A. Kokhanovsky), 3, 1-26, Praxis-Springer, 2008.

480 J. Hansen, and L. Nazarenko, 2004: "Soot climate forcing via snow and ice albedos", *Proc.*
481 *Natl. Acad. Sci.*, 101, 423-428, doi:10.1073/pnas.2237157100, 2004.

482 B. Hapke, *Theory of reflectance and emittance spectroscopy*, Cambridge: Cambridge University
483 Press, 2005.

484 C. He, K.-N. Liou, Y. Takano, P. Yang, L. Qi, and F. Chen, "Impact of grain shape and multiple
485 black carbon internal mixing on snow albedo: parameterization and radiative effect analysis", *J.*
486 *Geophys. Res.*, 123, 1253-1268, 2018.

487 A. A. Kokhanovsky, E.P. Zege, "Scattering optics of snow", *Appl. Optics*, vol. 43, N7, pp.1589-
488 1602, 2004.

489 Q. Libois, G. Picard, M. Dumont, L. Arnaud, C. Sergent, E. Pougatch, M. Sudul, and D. Vial, "
490 Experimental determination of the absorption enhancement parameter of snow", *J. Glaciology*,
491 60, N 222, 2014.

492 Q. Libois, G. Picard, L. Arnaud, M. Dumont, M. Lafaysse, S. Morin, and E.
493 Lefebvre, "Summertime Evolution of Snow Specific Surface Area close to the Surface on the
494 Antarctic Plateau," *The Cryosphere*, 9, N6, 2383-2398, 2015.

495 S. McKenzie Skiles, T. Painter, G. S. Okin, "A method to retrieve the spectral compex refractive

496 index and single scattering optical properties of dust deposited in mountain snow'', J.
497 *Glaciology*, 63, N237, 133-147.

498 M. I. Mishchenko, J.M. Dlugach, E.G. Yanovitskij, and N.T. Zakharova, "Bidirectional
499 reflectance of flat, optically thick particulate layers: An efficient radiative transfer solution and
500 applications to snow and soil surfaces", *J. Quant. Spectrosc. Radiat. Transfer*, vol. 63, pp. 409-
501 432, doi:10.1016/S0022-4073(99)00028-X, 1999.

502 Y. Nazarenko, S. Fournier, U. Kurien, R. B. Rangel-Alvarado, O. Nepotchatykh, P. Seers, P. A.
503 Ariya, "Role of snow in the fate of gaseous and particulate exhaust pollutants from gasoline-
504 powered vehicles". *Environmental Pollution*, 223, 665 DOI: 10.1016/j.envpol.2017.01.082,
505 2017

506 G. Picard, Q. Libois, L. Arnaud, G. Verin, and M. Dumont, "Development and calibration of an
507 automatic spectral albedometer to estimate near-surface snow SSA time series." *The
508 Cryosphere*, 10, N3, 1297-1316, 2016.

509 K. Stamnes, B. Hamre, J. J. Stamnes, G. Ryzikov, C. Biryulina, R. Mahoney, B. Haus, and A.
510 Sei, "Modeling of radiation transport in coupled atmosphere-snow-ice-ocean systems", *J.
511 Quant. Spectrosc. Radiat. Transfer*, 112, 714-726, 2011.

512 N. Utry, T. Ajtai, M. Pinter, E. Tombacz, E. Illes, Z. Bozoki, and G. Szabo, "Mass-specific
513 optical absorption coefficients and imaginary part of the complex refractive indices of mineral
514 dust components measured by a multi-wavelength photoacoustic spectrometer", *Atmos. Meas.
515 Techniques*, 8, 401-410, 2015.

516 H. C. Van de Hulst, *Light scattering by small particles*, N.Y: Dover, 1981.

517 S. G. Warren, W. J. Wiscombe, "A model for spectral albedo of snow: II. Snow containing
518 atmospheric aerosols", *J. Atmos. Sci.*, vol. 37, pp. 2734-2745, 1980.

519 S. G. Warren, "Can black carbon in snow be detected by remote sensing", *J. Geophys. Res.,
520 Atmospheres*, 118, 779-786, 2013.

521 T. Weil, C. De Filippo, D. Albanese, C. Donati, M. Pindo, L. Pavarini, and F. Miglietta, "Legal
522 immigrants: invasion of alien microbial communities during winter occurring desert dust
523 storms", *Microbiome*, vol. 5, No 1, <https://doi.org/10.1186/s40168-017-0249-7>, 2017.

524 W. J. Wiscombe, and S. G. Warren, "A model for spectral albedo of snow: I. Pure snow", *J.
525 Atmos. Sci.*, vol. 37, pp. 2712-2733.

526 E. P. Zege, I. L. Katsev, A. V. Malinka, A. S. Prikhach, G. Heygster, and H. Wiebe, "Algorithm
527 for retrieval of the effective snow grain size and pollutants amount from satellite
528 measurements", *Rem. Sens. Env.*, 115, 2674-2685.

529

530

531 Tables

532

533 Table 1. The derived snow parameters for the five samples. The value of c is assumed to be equal

534 1/3, which leads to the extinction length ($l_{ext} = 1/\kappa_{ext}$) to be equal to the effective grain diameter

535 d . The absorption coefficient is given at the wavelengths $\lambda_0 = 1000\text{nm}$ and $\lambda^* = 560\text{nm}$.

536	N	$\kappa_{abs}^{pol}(\lambda_0), m^{-1}$	$\kappa_{abs}^{pol}(\lambda^*), m^{-1}$	m	d, mm	Site
537	1	0.0182	0.1954	4.1	2.1	Col du Lautaret (site 1)
538	2	0.0342	0.2668	3.5	2.2	Col du Lautaret (site2)
539	3	0.1073	0.7194	3.3	1.7	Col du Lautaret (site 3)
540	4	0.0769	0.5324	3.3	1.9	Col du Lautaret (site 4)
541	5	0.0943	0.3848	2.4	2.2	Col du Lautaret (site 5)
542	6	0.0111	0.1191	4.1	2.5	Artavaggio plains (site 1)
543	7	0.0077	0.3123	6.4	1.5	Artavaggio plains (site 2)

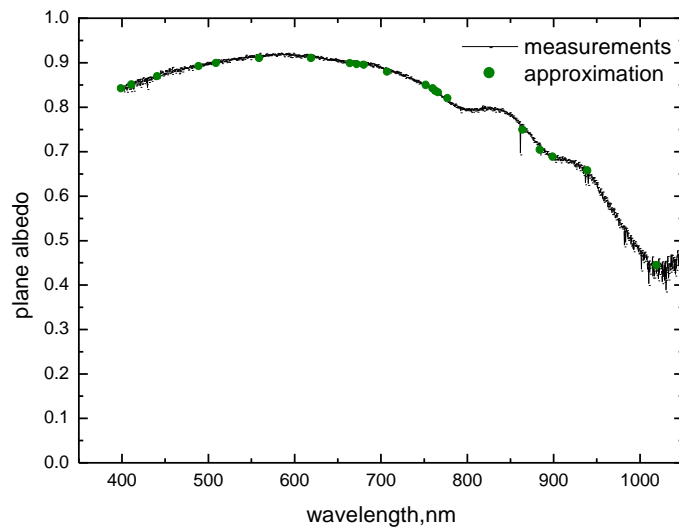
544

545

546

547

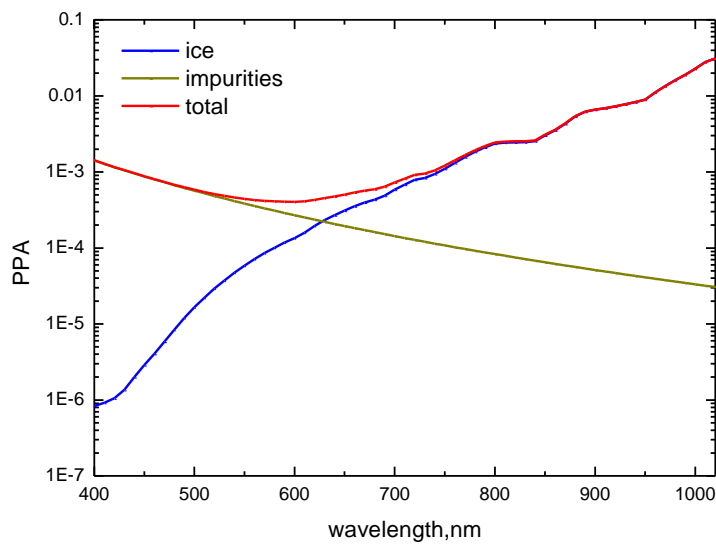
548 Figures



549

550 Fig.1. The intercomparison of theory (symbols) with experimental measurements of plane albedo
551 (line, no noise removed) performed in French Alps ($45^{\circ}2' N$, $6^{\circ}2' E$, 2100 m a.s.l.) obtained on
552 12/04/2017. The plane albedo is an average of 5 measurements performed between 08h55 and
553 09h30 UTC for a polluted (by dust) snowpack. The solar zenith angle for the measurements was
554 between 47° and 49° . The noise of measurements has not been removed and clearly seen in the
555 near infrared portion of the spectrum.

556

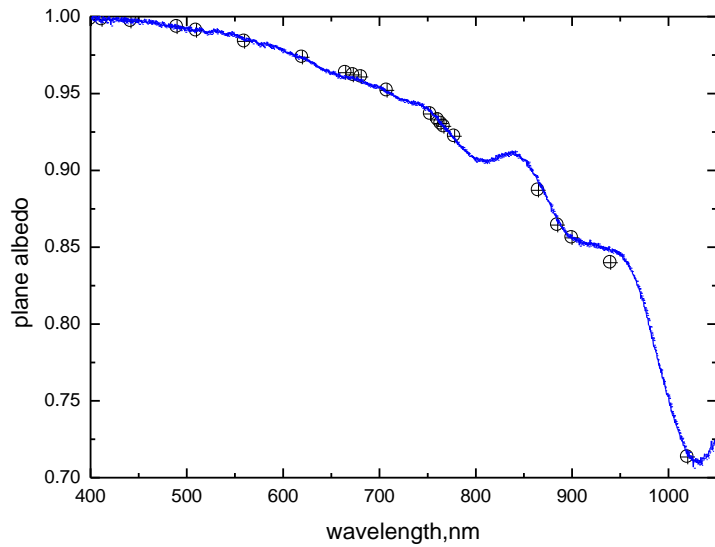


557
558

559 Fig.2. The derived spectral probability of photon absorption for the case presented in Fig.1.

560

561

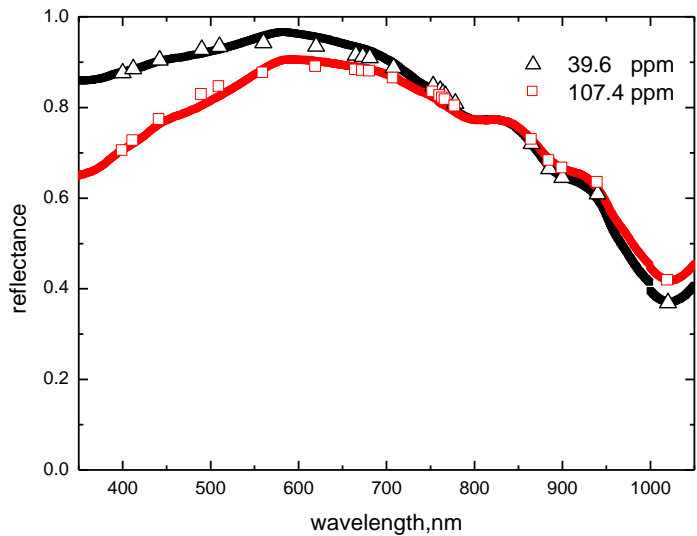


562
563

564 Fig.3 The inter-comparison of theory (symbols) with experimental measurements of plane albedo
565 (line) performed in Antarctica (Dome C, $75^{\circ}5'$ S, $123^{\circ}17'$ E) for pure snow. The measured plane
566 albedo was obtained on 10/01/2017 at 23h24 UTC, for a solar zenith angle of 63 degrees. The
567 parameters l, f, m have been derived from the measurements at 400, 560, and 1020nm.

568

569



570

571 Fig.4 The inter-comparison of theory (symbols) with experimental measurements (line) in
572 European Alps ($45^{\circ}55'56.70''N$; $9^{\circ}31'33.28''E$) for the polluted snowpack. The parameters R_0 , l ,
573 f , m have been derived from the measurements at 400, 560, 865 and 1020nm.
574 Reflectance measurements were collected on snow containing different concentration of dust:
575 39.6 ppm (black line) and 107.4 ppm (red line). The dust has been collected from the upper snow
576 layer (≈ 5 cm). Snow was clean at larger depths. A complete description of this dataset is
577 presented in Di Mauro et al. (2015).

578